High Speed and Low Cost One-to-Many VLC Using Polymer-Dispersed Liquid Crystals

Yuehu Jiang†, Haonan Wu†, Yi-Chao Chen†* , Guangtao Xue†‡
†Department of Computer Science and Technology, Shanghai JiaoTong University, China
‡Shanghai Key Laboratory of Trusted Data Circulation and Governance in Web3
{jiangyuehu, haonanwu, yichao, xue-gt}@sjtu.edu.cn

***Abstract*—Visible light communication (VLC) is considered a solution to the scarcity of radio frequency communication resources due to its abundant spectrum resources and rapid intensity modulation capability. It has a wide range of applications in indoor positioning and intelligent transport systems. For example, in Connected and Autonomous Vehicle scenarios, VLC uses traffic lights to warn vehicles at different distances in abnormal situations, thus preventing potential traffic accidents. To facilitate fast, long-range VLC communication in such one-to-many communication scenarios, current systems typically use optical cameras or digital micro-mirror devices as receivers. However, there are several challenges associated with these devices. Optical cameras have a limited sampling rate, resulting in reduced effective throughput. Other receivers, such as digital micro-mirror devices, are relatively costly, which hinders their widespread use.**

In this paper, we propose a novel, low-cost, and high-speed VLC scheme. We use a low-cost material called Polymer-Dispersed Liquid Crystal as the measurement matrix, reducing the cost by 99% compared to digital micro-mirror devices. We implement hierarchical coding based on compressive sensing to reduce data redundancy and thus improve communication throughput. Empirical experiments conducted using four photodiodes at the receiver show a 120% improvement in overall throughput compared to existing one-to-many VLC systems.

***Index Terms*—visible light communication, hierarchical coding, compressive sensing**

I. Introduction

Connected and autonomous vehicles (CAVs) are emerging as a key development in Intelligent Transport Systems (ITS). These vehicles can communicate with each other and with infrastructure elements in real time, facilitating the exchange of information to improve traffic efficiency and safety. For example, as demonstrated in Fig. 1, a traffic light transmits live traffic conditions to nearby vehicles. This scenario, where one source communicates with multiple receivers, requires fast communication speeds to keep up with the rapidly changing environment. While many current approaches rely on Radio Frequency (RF) technology, this method faces challenges in dense areas where bandwidth is shared among numerous users, resulting in considerable interference, reduced system capacity, and increased latency. Consequently, Visible Light Communication (VLC) is gaining traction as a complementary technology to RF in outdoor and vehicular communication [1], offering several advantages that address the limitation of RF [2].

*Corresponding author

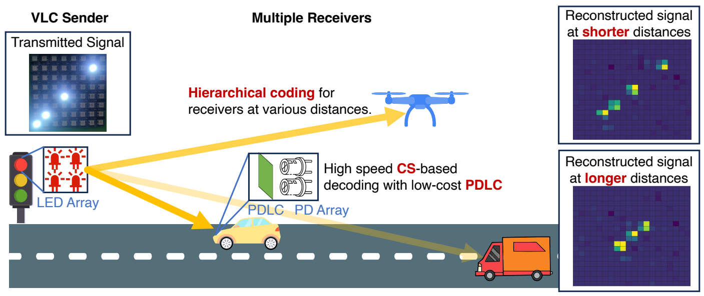

Fig. 1. In a one-to-many intelligent traffic communication system, a CS-based hierarchical coding scheme used by PDLC allows receivers at different communication distances to reconstruct signals at different levels, thereby accessing different amounts of information.

In addition to CAVs, the widespread use of LED lighting in buildings promotes the implementation of various location-aware indoor applications [3], [4]. To fit different communication scenarios, VLC utilizes various receivers, typically including photodiodes (PDs) and cameras. PDs can provide high sampling rates, while cameras offer spatial modulation capabilities by utilizing a two-dimensional sampling plane.

Nevertheless, communication distance remains a key limiting factor in the above-mentioned applications. Over longer ranges, communication systems often experience severe inter-channel interference, a consequence of the Rayleigh criterion [5]. This is particularly evident in one-to-many communication setups, as ensuring that data is received at different distances usually requires receivers near the source to sacrifice their data rates for the benefit of receivers further away. Numerous studies have attempted to address this issue. For example, OnionCode [6] proposes a multi-priority receiving approach that enables receivers to dynamically discard lower-priority bitstreams based on the evaluated channel capacity. However, this hierarchical encoding method is primarily reliant on the camera, resulting in the transmission of a substantial amount of redundant pixels. Additionally, the frame rate of cameras poses a significant limitation on the data transmission rate in these methods. Alternatively, Raytrack [7] employs Digital Micro-mirror Devices (DMD) and compressive sensing (CS) algorithms for fast transmitter detection. While DMDs offer a higher sampling rate, their use incurs considerable costs and increased power consumption. Furthermore, this approach does not effectively address the problem of reduced data rates for receivers at shorter distances, which is a compromise made to accommodate receivers at longer ranges.

To address the aforementioned issues, we utilize CS to implement a multi-priority hierarchical coding scheme in PD-based VLC. Our aim differs from that of traditional single-pixel imaging, which concentrates on reconstructing high-quality images. Instead, our objective is limited to roughly determining the position and intensity of the transmitters. Rather than employing DMD, we exploit a custom measurement matrix using low-cost Polymer-Dispersed Liquid Crystals (PDLCs). The hierarchical coding scheme based on CS and facilitated by PDLCs enables higher communication throughput and lower costs.

The use of PDLC smart glass allows for widespread application of our work in various scenarios, including indoor settings and intelligent transportation, as demonstrated in Fig. 1. Our work's primary contribution can be summarised as follows:

- A power-efficient and low-cost measurement matrix is designed using PDLCs, which are widely employed.
- A hierarchical coding scheme with multiple priorities was implemented using PD-based VLC, resulting in a significant increase in communication throughput.
- Specific experiments are designed to evaluate the impact of configurations and different algorithms on the system's performance.

Our paper is structured as follows: Sec. II provides a review of existing work in the field. Sec. III introduces the background and preliminary studies that underpin our research. The detailed design of our system is presented in Sec. IV. We discuss experimental results from our testbed in Sec. V, and finally, Sec. VI concludes the work.

II. Related Work

A. VLC with PD

Due to the higher sampling rate and lower cost of photodiodes (PDs) compared to cameras, much research has been focused on enhancing communication distance and improving the performance of PD-based VLC. [8] uses a combination of a DMD and a mirror assembly as a transmitter. The DMD determines the reflection of the incoming light and directs it to a proper receiver. [7] utilizes the DMD to detect the transmitter's position and dynamically adjusts the field of view (FOV) in real time, mitigating interference originating from the environment and other coexisting transmitters.

Our research employs Polymer-Dispersed Liquid Crystal (PDLC) to create a measurement matrix, instead of using expensive DMDs. This substitution results in lower power consumption and reduced cost.

B. Hierarchical Coding

In camera-based VLC, hierarchical coding is often used to improve communication distance. One example of this is Nishimoto's approach [9], [10], which involves dividing the LED array into blocks of different sizes that correspond to different priorities or layers. These blocks contain embedded bits of different layers that are overlaid together to generate the overlay code. Another approach is Onioncode [6], which uses a unique non-block-based coding scheme to maximize channel utilization. Onioncode does not compromise the data rate of the closest receiver and significantly enhances the overall throughput in one-to-many communication scenarios.

In comparison to the current hierarchical coding system that is based on cameras, we use PDs as receivers to improve the sampling rate and increase throughput.

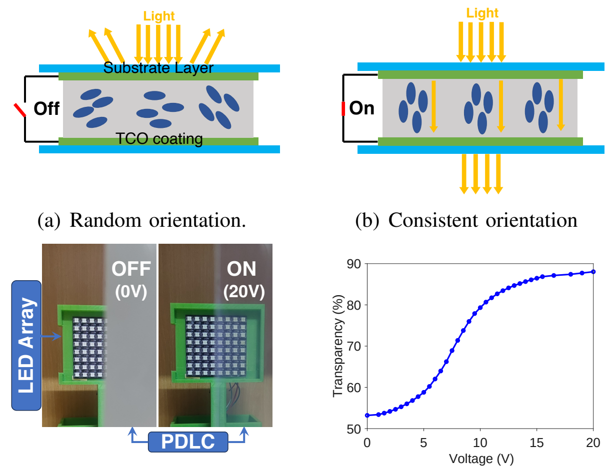

(a) Random orientation. (b) Consistent orientation

(c) Two states of PDLC. (d) Varying voltage.

Fig. 2. PDLC: (a) When the liquid crystals have random orientation, PDLC is opaque. (b) When the liquid crystals have a consistent orientation, PDLC becomes transparent. (c) Examples of PDLC at two states. (d) Transparency under varying voltage.

III. Background & Preliminary

A. Polymer-Dispersed Liquid Crystals

Polymer-Dispersed Liquid Crystals (PDLC) are a unique type of liquid crystal material composed of low molecular weight nematic liquid crystals dispersed as microdroplets in a polymer matrix (0.5-1μm). The random distribution of liquid crystals in the polymer matrix increases the material's haze, resulting in opacity. This material can transition from a non-transparent to an optically transparent state when subjected to an electric field. The liquid crystal droplets align along the field direction, with a control voltage typically ranging from 20-80V. The response time is typically less than $1ms$ [11]. Smart films or glasses, also known as smart or switchable windows, can be made by sandwiching such components between two transparent conductive oxide (TCO)-coated polyethylene terephthalate (PET) sheets [12]. Currently, most smart PDLC windows are self-adhesive laminated films used for privacy control in areas such as conference rooms and critical care areas.

The optical transparency characteristics were evaluated at different voltages. Fig. 2(d) shows that the transparent film is opaque with a transparency of about 53% when there is no control voltage and becomes transparent when the control voltage increases from $0V$ to $20V$. Due to its ease of control and processing, low cost, energy efficiency, and wide application in daily life, we choose PDLC to construct the measurement matrix.

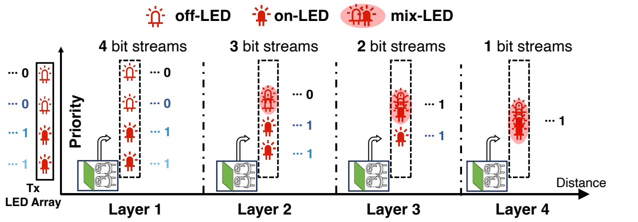

Fig. 3. Varying communication distances result in different levels of LED mixing and corresponding changes in light intensity. This phenomenon is harnessed to develop the hierarchical coding scheme.

B. Compressive Sensing

Unlike traditional signal processing, which assumes that a signal must be sampled uniformly at or above its Nyquist rate to be accurately reconstructed, Compressive Sensing (CS) is a technique that allows for accurate reconstruction with fewer samples [13]. If a signal is sparse or compressible in an orthonormal basis and the transformation basis and measurement matrix are incoherent, CS can acquire and reconstruct the signal with fewer measurements than required by the Nyquist-Shannon sampling theorem [13].

Mathematically, consider a real-valued signal vector x of length N to be recovered. Assume that x is a K-sparse signal in the basis of $\Psi = [\psi_1|\psi_2|\cdots|\psi_N]$, then x can be expressed as Eq. (1):

$$x = \sum_{i=1}^{N} \alpha(i)\psi_i = \Psi\alpha, \tag{1}$$

where Ψ is an $N \times N$ matrix with ψ_i as $N \times 1$ columns and α is an $N \times 1$ coefficient vector with K nonzero elements. By M times linear measurements which are properly designed ($M > N$), the $M \times 1$ measurement intensity vector y can be expressed as Eq. (2):

$$y = \Phi x = \Phi\Psi\alpha, \tag{2}$$

where the $M \times N$ measurement matrix Φ is incoherent to Ψ. Solving α to recover x is a convex optimization problem known as basis pursuit (BP) [14]. It has been proved that BP can be solved using l_1-minimization shown by Eq. (3) [13], [15]:

$$\min_{\alpha} \|\alpha\|_1 \ s.t. \ y = \Phi\Psi\alpha. \tag{3}$$

Considering noise is inevitable to measure y in practical use cases, BP can be modified to be basis pursuit denoising (BPDN) shown by Eq. (4) [16]:

$$\min_{\alpha} \frac{1}{2}\|y - \Phi\Psi\alpha\|_2^2 + \lambda\|\alpha\|_1 \ s.t. \ y = \Phi\Psi\alpha, \tag{4}$$

where λ is modified to trade off reconstruction error in the first term with the sparsity of α in the second term.

C. Hierarchical Coding

As the distance between the LED and the photodiodes (PDs) increases, the ability of CS to spatially differentiate closely situated LED light sources diminishes. This phenomenon is known as LED spatial mixing, as illustrated in Fig. 3. However, this mixing results in a more intense light output. We can exploit this characteristic to devise a hierarchical coding scheme, where spatially mixed LEDs are treated as a singular signal and encoded individually at each layer[1].

Notably, receivers at longer distances may not be able to distinguish individual lit LEDs, but they can perceive the total number of LEDs illuminated during LED mixing. Therefore, each instance of LED mixing is linked to a specific communication layer and a unique decoding table. For instance, in Fig. 3, Layer3 involves three adjacent LEDs undergoing mixing, which the receiver interprets as a single-lit LED. Using a decoding table, the second-priority bit is decoded as '**1**'. This ensures that high-priority bits remain decodable at longer distances while preserving full bandwidth for closer receivers.

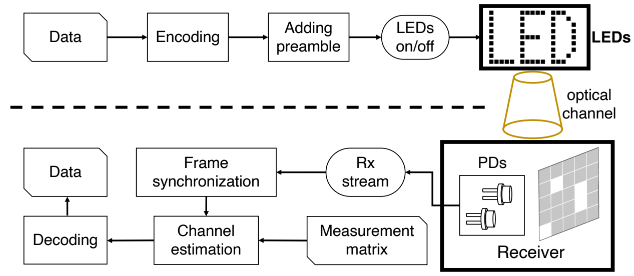

Fig. 4. Architecture of PDLC-CS-based VLC system.

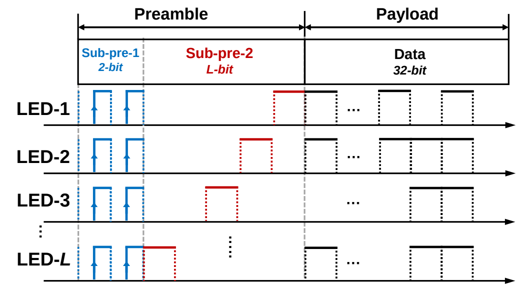

Fig. 5. Frame structure.

IV. System Design

A. System Overview

We develop a proof-of-concept PDLC-CS-base VLC system. Fig. 4 illustrates the architecture, which consists of an LED array as the transmitter and several photodiodes (PDs) with a Polymer-Dispersed Liquid Crystal (PDLC) measurement matrix serving as the receiver.

B. Transmitter Design

The information source generates bit streams which are then framed at the transmitter using a customized preamble. The frame structure of our communication system is illustrated in Fig. 5. Each frame contains 32 data bits and a customized preamble consisting of 2 sub-preambles. *Sub-preamble-1* and *2* are specifically designed for frame synchronization and optical channel estimation, respectively. We use the baseband transmission method with NRZ line code to validate the effectiveness of our system.

[1]Each layer corresponds to a specific range of distances

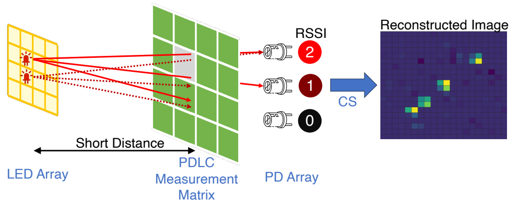

(a) The receiver is closer and the reconstructed image has a higher resolution.

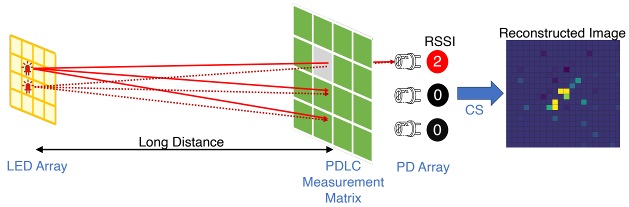

(b) The receiver is further and the reconstructed image has a lower resolution.

Fig. 6. (a) When the receiver is located near the LED array, the nearby LEDs can be sampled differently using the PDLC measurement matrix. This leads to a distinguishable signal upon reconstruction. (b) When the receiver is located far away from the LED array, the nearby LEDs are likely to be sampled by the same PDLC element. This leads to less information for CS reconstruction, resulting in a lower resolution.

C. Receiver Design

1) Initialization: The communication system is established using x LEDs and p PDs, with a PDLC measurement size of $m \times m$. To initialize the receiver, sparse measurement matrices are generated, each with dimensions of $m \times m$ and elements of **0** and **1** to represent the opaque and transparent states of the corresponding PDLC glass cell. Fig. 6 illustrates how different cell states affect the received signal. The PDLC measurement matrix contains cells that establish a line of sight (LOS) with the PD from a sampling point. There are a total of $p \cdot m \cdot m$ sampling points. As we are only concerned with the sampling points in the LED array, we can assume that they all lie within the plane of the array. Their relative positions can then be calculated using spatial geometric operations.

Measurement Matrix Design: For effective use of CS in image reconstruction, the measurement matrix must adhere to the Restricted Isometry Property (RIP) [13]. However, verifying the RIP characteristic of a measurement matrix in practice can be challenging. This often leads to the use of a random matrix as an approximation, which may not always yield optimal results. To address this issue, We propose a *pre-learned* measurement matrix generation algorithm. Based on preliminary experiments, we identify cells that are frequently traversed by the line of sight (LOS). We then generate matrices to ensure a more uniform distribution of **0**' and **1**' elements across these cells. This strategy helps prevent any individual cell from persistently remaining in an 'on' or 'off' state during the sampling process.

Image Reconstruction with CS: Based on preliminary experiments, we compute an angular attenuation matrix of size $m \times m$ for each PD. The PDLC measurement matrix transforms during the sampling process, with the frequency of f referred to as the **transformation rate**. This generates a transparency array of size $m \times m$. The complete measurement matrix, denoted as Φ, has dimensions $f \cdot p \times p \cdot m \cdot m$ and is formed by taking the Hadamard product of the transparency matrix and the angular attenuation matrix. The output, y, from f samplings is represented as a vector of size $f \cdot p \times 1$. Therefore, the mathematical expression for the communication model is as follows:

$$y = \Phi \alpha \tag{5}$$

After deriving Φ, we exploit the *L1eq_pd* function in *l1-magic* [17] to solve the BPDN equations and obtain α for further channel estimation.

2) Frame Synchronization: The sub-preamble-1 is designed for frame synchronization and consists of 2 repeated Manchester bits. As illustrated in Fig. 7, at the receiver, received signal streams are divided into f groups by extracting signals sampled through the same PDLC measurement matrix. A filter matching the sub-preamble-1 is used for cross-correlation calculation for each group. The preamble start can be identified based on the first maximum cross-correlation.

3) Optical Channel Estimation: After synchronizing the frames, we detect the number of mixed LEDs to determine the communication layer and encoding table. In sub-preamble-2, LEDs light up sequentially, and the receiver uses CS to construct vector α in Equation 5. The values of the elements in the vector represent the luminance at the sampling points. The vector α is then transformed back into a 2-D matrix and its elements are distributed onto a plane according to their relative positions, as computed in Section IV-C1. To eliminate noise and extract LED positions, simple filtering, and threshold segmentation are used. Fig. 8 shows that when sampling points from different LEDs overlap, LED-mixing occurs. The communication layer is determined based on the number of overlapping LEDs. Finally, pre-measurement is used to determine the intensity corresponding to different numbers of illuminated LEDs. The source information can then be decoded based on the channel estimation results.

V. Evaluation

As shown in Fig 9, we use WS2812B [18] as the system's transmitter, use SGPN185MQ [19] as the receiver, and cut Polymer-Dispersed Liquid Crystal (PDLC) films into $1cm \times 1cm$ panes to assemble into the measurement matrix.

A. Benchmark

1) Preamble Detection: The first step is to assess the robustness of the frame synchronization. We define **frame detection accuracy** as the proportion of correctly identified frames. Fig. 11 illustrates the frame detection accuracy under different lighting conditions and with varying numbers of PDs. '**Indoor**' refers to a standard office with light-on, while '**Outdoor**' indicates natural sunlight outdoors. The experiments show that the frame detection rate indoors can reach 99.0%-99.6% with 1 to 4 PDs, while outdoors, due to strong sunlight interference, the detection rate drops to 92.2%-93.8%.

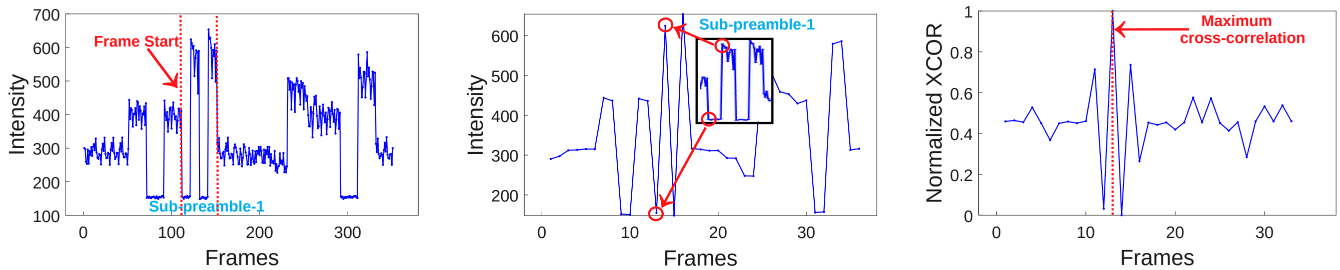

(a) Received signal stream at the receiver. (b) Extracted signal stream from sub-pre-1. (c) Cross-correlation of extracted signal stream.

Fig. 7. Process of frame synchronization.

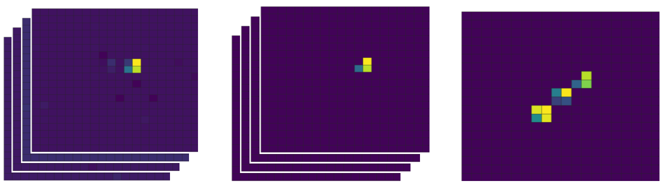

(a) Reconstructed signal of sampling points. (b) Filter and threshold segmentation. (c) Layer and channel estimation.

Fig. 8. Process of channel estimation.

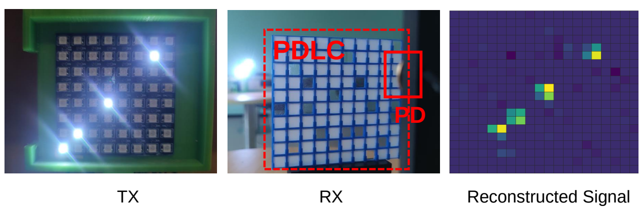

Fig. 9. System prototype.

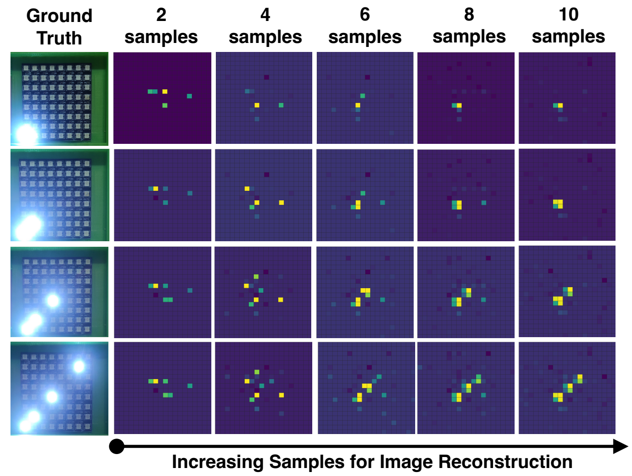

Fig. 10. Reconstructed images while varying the number of samples.

2) Measurement Matrix: The quality of image reconstruction is heavily influenced by the measurement matrix. To assess the impact of three key factors - **transformation rate**, **sparsity**, and the **transformation generation algorithm** - we use reconstruction accuracy as our performance metric. Reconstruction accuracy is defined as the ratio of correctly decoded images to reconstructed images.

We begin by analyzing the effect of the **transformation rate**. After each transformation of the PDLC measurement matrix, PDs collect a sample. As depicted in Fig. 10, it is evident that an increase in the number of samples collected results in more precise image reconstruction through CS.

Next, we examine the impact of **sparsity**. Measurement matrices with varying sparsity levels are randomly generated and tested with different sample counts. Fig. 12 reveals two key observations. First, for a given sparsity level, reconstruction accuracy improves by 24.1%, from 74.7% to 98.8%. Second, while higher sparsity levels allow for more comprehensive information collection, they also increase reconstruction complexity. At low transformation rates, sparsity has little impact. However, increasing the transformation rate can flexibly adapt to different scenarios, balancing communication speed and reconstruction accuracy. This adaptability makes our PDLC-CS-based VLC system suitable for diverse environments.

Fig. 13 examines the effect of different **algorithms on the generation of measurement matrices**. We contrast matrices that are **pre-learned** with those that are **randomly generated**. The findings indicate superior performance from the pre-learned algorithm. Remarkably, as the sample count increases, even randomly generated matrices can achieve performance almost as good as pre-learned ones, with accuracy reaching close to 98.5%.

B. Overall Performance

1) System Throughput: A comparison was conducted between communication systems with and without hierarchical coding schemes. Fig. 14 demonstrates the results. The throughput of $Layer1$, where LED-mixing does not occur, was normalized to 1. The hierarchical coding scheme allows for the transmission of additional data through LED-mixing. In the 4-layer coding system, the overall throughput of the communication system increases by approximately 42.8%.

We also compare our method with OnionCode [6] which is the state-of-the-art hierarchical coding scheme in one-to-many visible light communication. As shown in Fig. 15, because of the high sampling rate of PDs, our PDLC-CS-based VLC scheme increases overall throughput by 120%.

2) Cost and Power Consumption: In addition to its high data rate, another key advantage of our method is its cost and energy effectiveness. As detailed in Table 16, compared to existing CS-based VLC schemes [7], [8] that typically employ Digital Micro-mirror Devices (DMD) at a cost of \$80 and $5W$ operating power [20], the PDLC glass we use are substantially more affordable, costing approximately $\$40/m^2$ with a power consumption of $8W/m^2$. The total area of our measurement matrix is less than $0.02m^2$. Therefore, both the cost and power consumption of our PDLC measurement matrix are significantly lower than those associated with DMDs. This

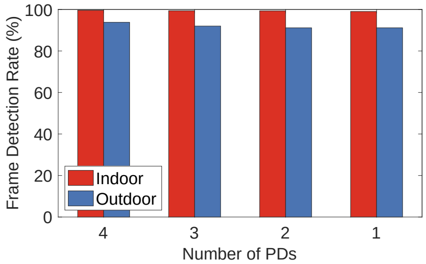

Fig. 11. Frame detection accuracy under different lightness.

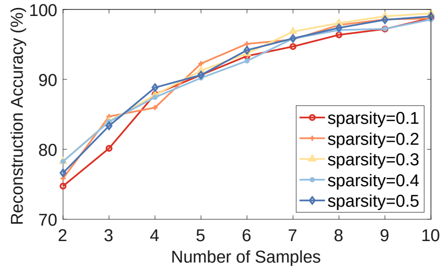

Fig. 12. Image reconstruction accuracy under different sparsity and transformation rate.

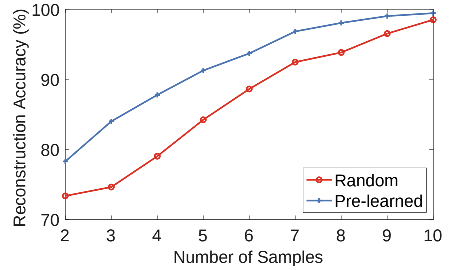

Fig. 13. Comparison of randomly generated matrix and pre-learned matrix.

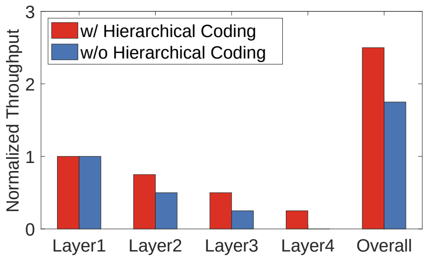

Fig. 14. Performance comparison between with and without the hierarchical coding scheme.

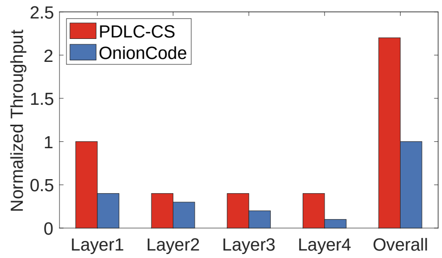

Fig. 15. Comparison between our PDLC-CS-based VLC and scheme from existing work (OnionCode).

	Price	Power	Num
DMD	$\geq$ \$80	$5W$	1
PDLC	\$$40/m^2$	$8W/m^2$	0.02

	Sample	Price	Num
Camera	$50Hz$	>\$15	1
PD	$10kHz$	\$9	4

Fig. 16. Cost comparison between DMD and PDLC, camera and PD.

makes our approach not only more economically viable but also more energy-efficient, making it suitable for a wide range of applications.

VI. Conclusion

This paper proposes a hierarchical coding scheme for one-to-many visible light communication scenarios based on photodiodes. The scheme utilizes polymer-dispersed liquid crystals to create a specialized measurement matrix for random sampling. Compressive sensing is employed to reconstruct signals from the light source and decode different priority bitstreams. The evaluation results show an overall increase in throughput of 120% and a reduction in cost of 99% compared to existing methods. The system is highly flexible and capable of adapting to various communication scenarios.

Acknowledgement

This work is supported in part by the NSFC under Grants 61936015, National Key R&D Program of China 2018YFB2101102, the Joint Key Project of the NSFC U1736207, and Program of Shanghai Academic Research Leader.

References

[1] Agon Memedi and Falko Dressler. Vehicular visible light communications: A survey. *IEEE Communications Surveys & Tutorials*, 2021.

[2] Parth H. Pathak, Xiaotao Feng, Pengfei Hu, and Prasant Mohapatra. Visible light communication, networking, and sensing: A survey, potential and challenges. *IEEE Communications Surveys & Tutorials*, 2015.

[3] Junhai Luo, Liying Fan, and Husheng Li. Indoor positioning systems based on visible light communication: State of the art. *IEEE Communications Surveys & Tutorials*, 19(4):2871–2893, 2017.

[4] Nasir Saeed, Haewoon Nam, Tareq Y. Al-Naffouri, and Mohamed-Slim Alouini. A state-of-the-art survey on multidimensional scaling-based localization techniques. *IEEE Communications Surveys&Tutorials*, 2019.

[5] Chun-Yu Chen, Bo-Yao Lin, Junding Wang, and Kang G. Shin. Keep others from peeking at your mobile device screen! *The 25th Annual International Conference on Mobile Computing and Networking*, 2019.

[6] Haonan Wu, Yi-Chao Chen, Guangtao Xue, Yuehu Jiang, Ming Wang, Shiyou Qian, Jiadi Yu, and Pai-Yen Chen. Onioncode: Enabling multi-priority coding in led-based optical camera communications. In *IEEE INFOCOM*, 2022.

[7] Wen-Hsuan Shen and Hsin-Mu Tsai. Raytrack: Enabling interference-free outdoor mobile vlc with dynamic field-of-view. In *Proceedings of ACM MobiSys*, page 376–388, 2021.

[8] Monia Ghobadi, Ratul Mahajan, Amar Phanishayee, Nikhil Devanur, Janardhan Kulkarni, Gireeja Ranade, Pierre-Alexandre Blanche, Houman Rastegarfar, Madeleine Glick, and Daniel Kilper. Projector: Agile reconfigurable data center interconnect. In *Proceedings of the 2016 ACM SIGCOMM Conference*, SIGCOMM '16, page 216–229, New York, NY, USA, 2016. Association for Computing Machinery.

[9] Sayaka Nishimoto, Tom Nagura, Takaya Yamazato, Tomohiro Yendo, Toshiaki Fujii, Hiraku Okada, and Shintaro Arai. Overlay coding for road-to-vehicle visible light communication using led array and high-speed camera. In *2011 14th International IEEE Conference on Intelligent Transportation Systems (ITSC)*, pages 1704–1709, 2011.

[10] Sayaka Nishimoto, Takaya Yamazato, Hiraku Okada, Toshiaki Fujii, Tomohiro Yendo, and Shintaro Arai. High-speed transmission of overlay coding for road-to-vehicle visible light communication using led array and high-speed camera. In *2012 IEEE Globecom Workshops*, 2012.

[11] V. Shibaev. Liquid crystalline polymers. In *Reference Module in Materials Science and Materials Engineering*. Elsevier, 2016.

[12] L. Niklaus, M. Schott, and U. Posset. Electrochromic windows. In *Reference Module in Chemistry, Molecular Sciences and Chemical Engineering*. Elsevier, 2023.

[13] D.L. Donoho. Compressed sensing. *IEEE Transactions on Information Theory*, 52(4):1289–1306, 2006.

[14] Shaobing Chen and D. Donoho. Basis pursuit. In *Proceedings of 1994 28th Asilomar Conference on Signals, Systems and Computers*, volume 1, pages 41–44 vol.1. 1994.

[15] E.J. Candes, J. Romberg, and T. Tao. Robust uncertainty principles: exact signal reconstruction from highly incomplete frequency information. *IEEE Transactions on Information Theory*, 52(2):489–509, 2006.

[16] Scott Chen, David Donoho, and Michael Saunders. Atomic decomposition by basis pursuit. *SIAM Journal on Scientific Computing*, 1998.

[17] L1-magic. https://candes.su.domains/software/l1magic/ Accessed November 1, 2023.

[18] WorldSemi. Ws2812b. https://cdn-shop.adafruit.com/datasheets/WS2812B.pdf Accessed November 1, 2023.

[19] Linear silicon photocell sgpn185mq silicon photodiode. https://dioded.com/p/linear-silicon-photocell-sgpn185mq Accessed November 1, 2023.

[20] Texas Instruments. Array products. https://www.ti.com/dlp-chip/display-and-projection/array/products.html Accessed November 1, 2023.